



ISSN: 0067-2904

Diabetes Diagnosis Using Deep Learning

Ali Hassan Khudair, Abdulkareem Merhej Radhi

Department of Computer Science, College of Science, Al-Nahrain University, Baghdad, Iraq

Received: 14/8/2022 Accepted: 19/2/2023 Published: 30/1/2024

Abstract

Hyperglycemia is a complication of diabetes (high blood sugar). This condition causes biochemical alterations in the cells of the body, which may lead to structural and functional problems throughout the body, including the eye. Diabetes retinopathy (DR) is a type of retinal degeneration induced by long-term diabetes that may lead to blindness. propose our deep learning method for the early detection of retinopathy using an efficient net B1 model and using the APTOS 2019 dataset. we used the Gaussian filter as one of the most significant image-processing algorithms. It recognizes edges in the dataset and reduces superfluous noise. We will enlarge the retina picture to 224×224 (the Efficient Net B1 standard) and utilize data augmentation methods to enhance the dataset photographs, and balance the dataset (which was quite uneven), to avoid overfitting. By using Transfer learning we save training time by using a previously learned deep CNN and transfer learning weights. In this research, EfficientNetB1 is compared against Xception, InceptionV3, MobileNet, and ResNet50 as a deep transfer learning model. The proposed model's accuracy, precision, recall, and f1-score are all examined. The EfficientNetB1 model outperforms all others in terms of overall testing accuracy (86.1%), sensitivity (87.24%), precision (97.6%), and F1-Score (89.32 percent). This approach might help physicians diagnose Diabetic Retinopathy earlier.

Key Words: Deep learning, Diabetic retinopathy, Efficient Net B1, Transfer learning, and Gaussian filter.

تشخيص داء السكري باستعمال التعلم العميق

علي حسن خضير ، عبد الكريم مرهج راضي

قسم علوم الحاسوب، كلية العلوم، جامعة النهرين، بغداد، العراق

الخلاصة

ارتفاع السكر في الدم هو أحد مضاعفات مرض السكري (ارتفاع نسبة السكر في الدم). تسبب هذه الحالة تغيرات كيميائية حيوية في خلايا الجسم، والتي يمكن أن تؤدي إلى مشاكل هيكلية ووظيفية في جميع أنحاء الجسم، بما في ذلك العين. اعتلال الشبكية السكري (DR) هو نوع من امراض الشبكية الذي يمكن أن يؤدي إلى العمى وينتج عن مرض السكري على المدى الطويل. قدمنا بحثاً عن العديد من الأساليب لتحديد اعتلال الشبكية السكري تلقائياً والسعي لاقتراح حل التعلم العميق الخاص بنا للتشخيص المبكر لاعتلال الشبكية من خلال استخدام نموذج EfficientNetB1 (وهو عبارة عن بنية CNN بها العديد من الطبقات العميقة). تم استعمال مجموعة بيانات APTOS 2019. يعد مرشح Gaussian أحد أهم تقنيات معالجة الصور. يكشف الحواف

ويزيل الضوضاء غير الضرورية من البيانات سنقوم بتغيير حجم صورة شبكية العين إلى 224×224 (معياري EfficientNetB1) واستعمال تقنيات زيادة البيانات لإثراء صور مجموعة البيانات وتحقيق التوازن بين مجموعة البيانات (لأنها كانت غير متوازنة للغاية) ومنع مشكلة فرط التجهيز. يستعمل التعلم الانتقالي شبكة CNN عميقة تم تدريبها بالفعل، وتحويل أوزان التعلم لتوفير وقت التدريب. كنموذج تعلم نقل عميق، تمت مقارنة EfficientNetB1 مع Xception و InceptionV3 و MobileNet و ResNet50 في هذه الدراسة. يتمتع نموذج EfficientNetB1 بأفضل testing accuracy شاملة (86.1%)، sensitivity (87.24%)، precision (97.6%)، F1-Score لجميع النماذج (89.32%). قد تساعد هذه الطريقة الأطباء في الكشف المبكر عن اعتلال الشبكية السكري.

1. Introduction

Hyperglycemia is a diabetic complication (high blood sugar). This disease produces a variety of biochemical changes in the body's cells, which can cause functional and anatomical issues throughout the body, particularly in the eye. Diabetes retinopathy (DR) is a type of retinal degeneration caused by long-term diabetes that can result in blindness. Diabetes is expected to impact 629 million individuals in the 20–79 age range globally by the end of 2045, a 48 percent increase from the present amount [1]. According to the World Health Organization (WHO), the most frequent type of diabetes is type 2, which arises when the body becomes insulin-resistant or does not generate enough insulin. Diabetic retinopathy is the result of a retinal blood vessel (BV) becoming damaged as a result of diabetes (DR). There are various symptoms of DR, including impaired vision, blank areas, and dark vision [2].

Diabetic retinopathy is divided into four stages:

- **Mild non-proliferative DR (NPDR):** At this stage, micro-aneurysms occur. There are little patches of balloon-like inflammation within the retina's small blood veins [3].
- **Moderate (NPDR):** At this stage, the blood veins that supply the retina are obstructed. There are also hemorrhages within the retina [4].
- **Severe (NPDR):** Retinopathy produces a loss of blood flow to the retina due to the obstruction of more blood vessels, signaling the retina to develop new blood vessels [5].
- **Proliferative (DR):** In this advanced stage of DR, new and aberrant blood vessels form on the retina's surface. These new blood vessels are fragile and prone to bleeding, resulting in a vision-threatening hemorrhage. They'll also convert to connective tissue, which will constrict over time, causing the retina to detach and result in blindness [6]. Figure (1) From fundus photos, instances of DR are based on the severity of the illness [7].

As a result, an accurate disease diagnosis is required. Methods of diagnosis such as fluorescein angiography and optical coherence tomography require the application of exogenous fluid or dye to the patient's eye after the retinal image is acquired [2]. Furthermore, occlusion, shadow, reflection, or inadequate lighting can degrade the quality of DR fundus pictures, making it difficult to distinguish between healthy and pathological areas [7]. However, for both physicians and patients, an automated system that can anticipate diabetic retinopathy without the need for an external agent is a more comfortable and easy way.

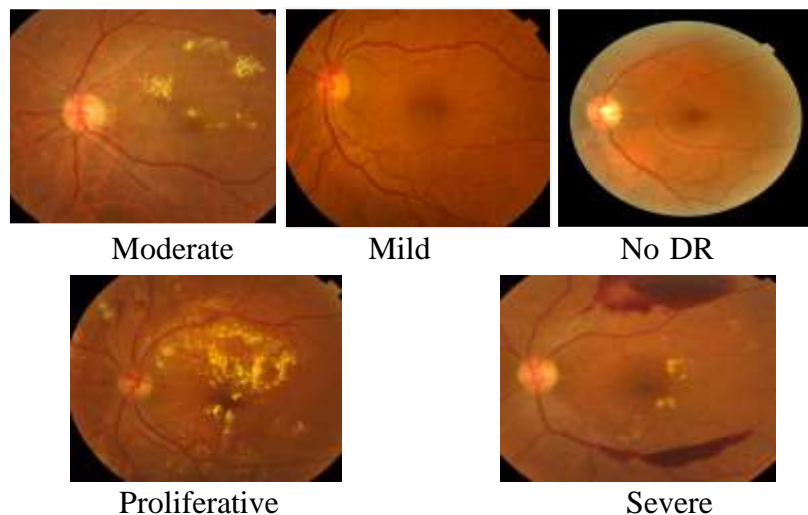


Figure 1 : instances of DR are based on the severity of the illness[8].

In recent years, computer vision applications, notably in the area of medical photo processing, have blossomed. Deep neural networks and other machine learning models have demonstrated promise in uncovering hidden patterns in a variety of datasets [9, 10]. Using deep learning methods to develop computer-aided diagnostic (CAD) systems that can identify abnormalities would help doctors improve patient care and judgments [11]. The rest of the paper is structured as follows: The second section contains initiatives in DR image categorization that are connected to the first. Section III outlines the material and the suggested method. The experimental analysis and discussion are presented in Section IV. The conclusions are presented in Section V.

2. Related Works

A review of existing techniques for DR diagnosis that use convolutional neural networks (CNNs) is provided.

In 2019, R. M. Sarki et al. [12] carried out studies with 13 convolutional neural network designs that were pre-trained utilizing the transfer learning approach on a large-scale ImageNet database. Several strategies for improving performance were used, including (i) fine-tuning, (ii) data augmentation, and (iii) volume growth. With ImageNet pre-training, ResNet50, XceptionNets, DenseNets, and VGG were trained and got the best accuracy of 81.3 percent.

In 2020, S. Sashank Sridhar et al. [3] quantified performance in recognizing different phases of the disease in humans using this technique, which builds a deep learning model using ResNet. Individual submodels for detecting the existence of diabetic retinopathy are built using ResNet and combined using the AdaBoost classifier. To identify the prognosis of the multiclass categorization of diabetic retinopathy, ResNet models are constructed and overlaid. Applied models had a performance accuracy of 78.88% for detecting the existence of diabetic retinopathy and 61.9 percent for evaluating the prognosis.

In 2016, H. C. Pratt et al. [13] employed an 11-layered ResNet model for learning using cost-sensitive learning and an over-sampling method with an upgraded dataset and attained an accuracy of around 80%.

In 2019, S. B. Shivashish Naithani et al. [14] created a CNN architecture capable of distinguishing detailed features in the retina with a sensitivity of 95% and an accuracy of 75%,

allowing for an automated diagnosis to determine severity.

In 2016, D. Doshi et al. [15] successfully used CNN on retinal fundus images for DR staging. Utilizing the transfer learning and contrast-limited adaptive histogram equalization approaches, they were able to obtain test and AlexNet model accuracy of 57.2 percent on 2-ary, 3-ary, and 4-ary classification models and 74.5 percent and 68.8 percent, respectively.

In 2017, S. Mohammadian et al [16] deep CNN has been used to develop a mechanism for automated disclosure of DR. It is based on a big dataset of roughly 35,000 photos. Images are scaled to 448x448 pixels in this project. also used some data enhancement techniques. Finally, the authors attained an accuracy of 81 percent for class 0 and 88 percent for class 1.

In 2017, S. A.-Z. Saad ALbawi et al [17] a technique for classifying DR into two groups: DR and No DR. A total of 35,126 pictures were used by the user, of which 20% were used to compare the algorithm's results against unreported data. The authors adjusted the two designs' last two blocks and compared two distinct optimizers with stochastic gradient descent, Adam, and different LR. The writers enhanced the photos by flipping them horizontally and vertically, twisting and shifting them to improve the system's accuracy. The accuracy of the InceptionV3 architecture is 87.12 percent, whereas the Xception architecture is 74.49 percent.

3. Materials and Methods

A. Proposed Approach

In numerous image identification and classification applications, convolutional neural networks (CNNs) [18] are utilized. A multilayer perceptron is the fundamental building block of every neural network [19]. The perceptron network is trained to reduce the discrepancy between observed and predicted results. A CNN differs from a straightforward neural network by having five primary layers:

- Fully Connected Layer.
- Input Layer.
- Output Layer.
- Pooling Layer.
- Convolutional Layer.

Deep convolutional layers are constructed in a variety of ways. AlexNet, LeNet, VGGNet, GoogleNet, and ResNet are among them.

The researchers Mingxing Tan and Quoc V. Le examine ConvNet scaling in detail and discover that properly balancing network width, depth, and resolution is a critical yet missing component that prevents improving efficiency and accuracy. Propose a simple but incredibly efficient compound scaling technique to overcome this challenge. enabled to swiftly increase a baseline ConvNet to any necessary resource restrictions while preserving model effectiveness. Demonstrate that a mobile-size EfficientNet model can be scaled up to achieve state-of-the-art accuracy by an order of magnitude fewer parameters, FLOPS, on both five regular and ImageNet-used transfer learning datasets [20]. Figure 2 shows the basic EfficientNet B1 architecture.

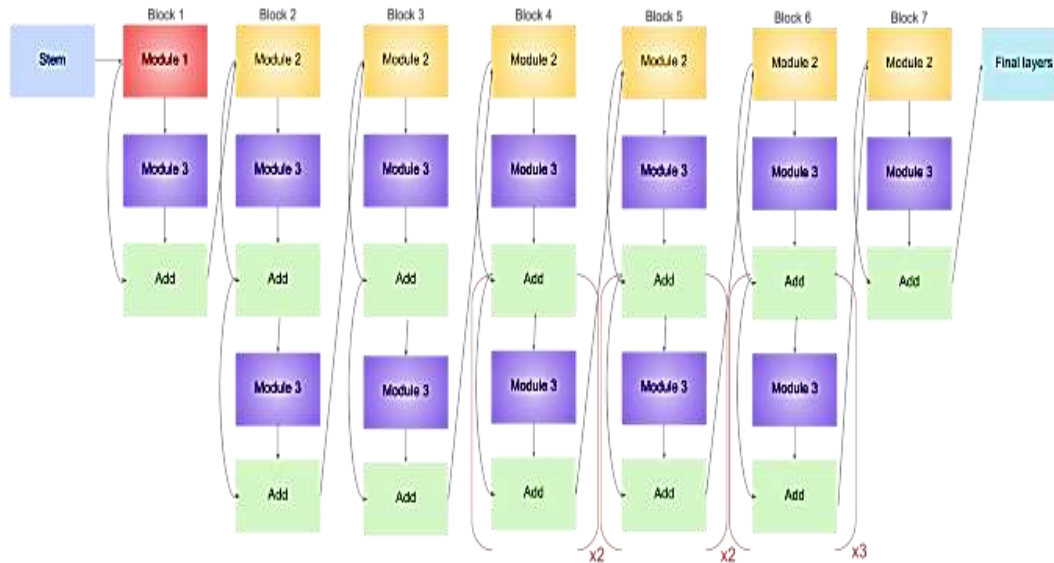


Figure 2 : EfficientNetB1 architecture [21].

In this paper, EfficientNetB1 is used to create a categorization system. Tan and Le [20] proposed the EfficientNet algorithm. The network was scaled using four different methods: width, depth, resolution, and compound scaling. Scaling up a baseline was straightforward. CNN will work around any resource limits. Because EfficientNetB1 contained 7.8 million parameters, we recommended using it to categorize the diabetic retinopathy datasets in our experiment. EfficientNetB1 had fewer parameters than DenseNet169, Xception, Inception-v3, and even ResNet-50.

In terms of performance, the proposed approach is compared to Xception architectures, ResNet50, Mobile Net, and InceptionV3. The following are the network structures of the chosen architectures:

-Xception: Francois Chollet was the first to propose the Xception architecture [22]. It's a continuation of the design from Inception. This architecture is made up of a linear stack of depth-wise separable convolution layers with residual connections. Memory use and objectives of depth-wise separable convolution Xception has 14 modules with 36 convolutional layers, all of which have linear residual connections except the first and last modules, which reduce processing time. In Xception, channel- and space-based information is learned via separable convolution. In addition, the residual link was constructed, which serves as a shortcut for resolving problems in the sequential network, including representational bottlenecks and fading gradients. This quick connection employs a summing operation in place of concatenation to allow the output of one layer to serve as the input for another.

-MobileNet: A Google research team created MobileNet [23], which has convolutional layers that can be separated by depth. In addition, with a minimal number of hyperparameters, the MobileNet architecture can achieve a high accuracy rate. The depth-wise separable convolution layers map the cross-channel and spatial correlations found in the input image feature maps. For a depth-wise separable convolution to function, two convolutions—one pointwise and one depth-wise—must be performed. Pointwise convolution ($1 * 1$) employs a filter for cross-channel patterns, and depth-wise convolution adds a single spatial filter to each input feature map. Standard convolutional layers capture both cross-channel and spatial patterns

at the same time, whereas separable convolutional layers separate the two patterns.

-Inception V3: Szegedy [22] proposed the Inception module, which has 42 levels. With 159 layers, Inception V3 is the third (3rd) iteration of Google Brain's Inception module. The basic idea behind the Inception module is to combine small and big kernels while reducing computational cost and parameter count to learn multi-scale representation. The deep residual learning network is responsible for first introducing the notion of a residual block (Res-Net).

-Res-Net50: The concept of a residual block (Res-Net) is first introduced by the deep residual learning network [22]. Residual blocks are utilized to connect the output of the second block to the input of the first block. The residual block uses this technique to learn the residual function and prevent parameter expansion. ResNet-50 is a 48-layer residual block architecture that includes a classifier layer with $1 * 1$ and $3 * 3$ small filters and a convolutional layer. The ILSVRC 2015 classification test, as well as the ImageNet and MS-COCO object identification contests, were all won by this design.

B. Overview of the Dataset:

The data used in this study comes from the APTOS 2019 diabetic retinopathy classification challenge, which can be accessed at [8]. Building machine learning models that can autonomously interpret fundus images for early diagnosis of DR is the goal of this challenge in rural areas where medical screening is difficult and time-consuming. The project also aims to develop machine learning models that can autonomously scan fundus images for the early identification of DR in rural areas where medical screening is challenging and time-consuming. The collection consists of 3662 fundus pictures of the retina collected at various clinics. There are 3662 fundus pictures of the retina in the collection, obtained at various clinics: moderate DR (class 2), proliferative DR (class 3), and severe DR (class 4). Table 1 illustrates the APTOS dataset's severely skewed class distribution.

Table 1: The percentage of each class in the APTOS dataset as well as its distribution of classes

Class	Label	Count	The ratio of the dataset's class
0	No DR.	1805	49.29 %
1	Mild DR.	370	10.10 %
2	Moderate DR.	999	27.28 %
3	Severe DR.	193	5.27 %
4	Proliferative DR.	295	8.06 %

C. Data Pre-Processing

Images were acquired in a variety of lighting circumstances, using various imaging instruments, and from a variety of clinics. As a consequence, the photographs in the collection vary in size, brightness, and, in some cases, focus. Preprocessing techniques were employed to address discrepancies and improve key characteristics.

•**The Gaussian filter:** a low-pass filter that operates in the frequency domain and is one of the most crucial methods in image processing. because noise has a high frequency. It has received a lot of attention in image processing and computer vision because the filter passes low frequencies. Although it is considered the best filter in several ways, there are some problems with it. A Gaussian filter is used to smooth out the noise while distorting the signal. The signal is distorted, but the noise is smoothed out with the use of a Gaussian filter. Edge detection using

a Gaussian filter as a preprocessor causes edge positions to vanish, cause displacement, and create phantom edges. When it comes to distinguishing frequencies, a Gaussian filter outperforms a monopolization filter. This operation is made easier by having an online windowed filter on hand. It is applied to an average image of 256 by 256 pixels, as long as the image is clean. Figure 3 contains examples of how the Gaussian filter works on retinal images. The filters and transform algorithms preserve smoother edges and more details while removing less noise from the photos. The noise variance rises, resulting in a drop in performance. By utilizing filters, you can eliminate noise from photographs and smooth them with the help of smoothing components. As a result, it's critical to reduce the image's high-frequency input so that it doesn't deteriorate; otherwise, the low-frequency input won't make a difference [24].

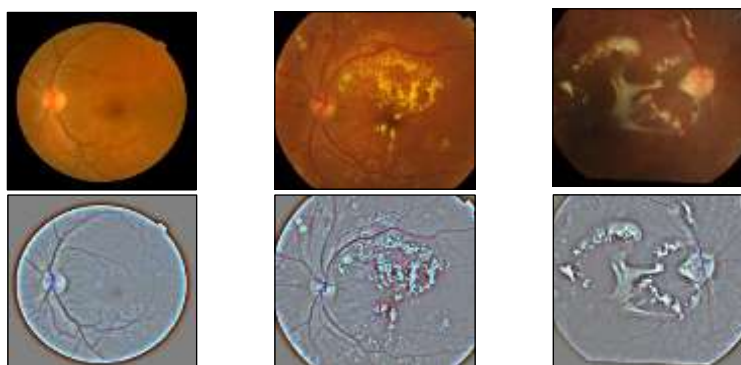


Figure 3: Original fundus photographs (top row) and photos that have been processed(bottom row).

- **Resizing:** The photographs acquired are also of various sizes and dimensions. The photos in the dataset are different in width and height. They must, however, be of the same size to be comparable. As a result, a picture resizing operation is necessary for this stage. Since EfficientNetB1 is used, which follows the aspect ratio, we expanded all of the images to (224×224) and then cropped them from the center to the final resolution of cubic interpolation to ensure that each retinal circle was in the center of the image.
-
- **Data augmentation:** Data augmentation is a popular method for boosting the number and variety of labeled training sets by modifying the input labels while keeping the output labels the same. To prevent overfitting in deep learning models, image augmentations are a common implicit regularization approach in computer vision. While most deep learning systems include basic image transformations, they are often limited to flipping, rotating, scaling, and cropping. Furthermore, the processing performance of existing picture augmentation packages varies [25]. Table (2) shows the number of images in the rows before and after the dataset was augmented.

Table 2 : Number of photos in the rows before and after data augmentation.

Class no	Label	Before augmentation	After augmentation
0	No DR.	1500	1500
1	Mild DR.	370	1500
2	Moderate -DR	999	1500
3	Severe DR.	193	1525
4	Proliferative DR.	295	1500

D. Performance Metrics

To assess the performance of the presented models, further performance matrices must be studied in this study. The two most popular performance measurements, accuracy and precision, are important concepts in DL, F1 score, and recall [26]. From equation (1) through equation (5), they are presented in sequence (4).

- **Accuracy:** is measured as the proportion of correctly categorized events to total occurrences.

$$\text{Accuracy} = \frac{TP+TN}{TP+TN+FP+FN} \tag{1}$$

- **Sensitivity or Recall:** Sensitivity is a measure of how many positive occurrences are favorably categorized [27].

$$\text{Recall} = \frac{TP}{TP+FN} \tag{2}$$

- **Precision:** is defined as the ratio of correctly recognized positive samples to the total number of positive samples correctly or mistakenly identified [28].

$$\text{Precision} = \frac{TP}{TP+FP} \tag{3}$$

- **F1-Score:** The arithmetic average of accuracy and recall is the F1-score.

$$\text{F1-Score} = 2 \times \frac{\text{Precision} \times \text{Sensitivity}}{\text{Precision} + \text{Sensitivity}} \tag{4}$$

Figure 4 below shows the four states of the confusion matrix, where TP stands for true positive samples, TN for true negative samples, FP for false positive samples, and FN for false negative samples [29].

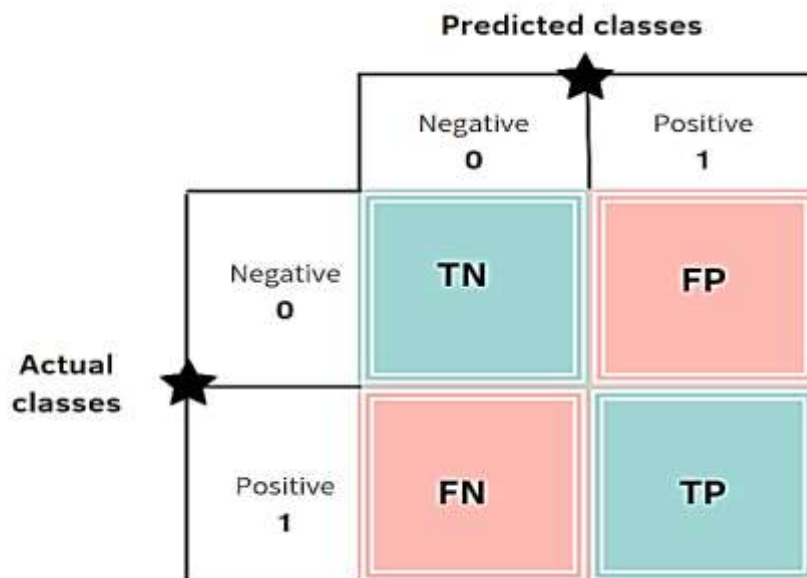


Figure 4 : Confusion Matrix [30].

4. Experimentations And Results

A. Setup For The Experiment

According to our data separation policy, the test set only receives 10% of the photos from each class, while the training set receives 80% of them. and the validation set is awarded 10%.

The pictures have been shrunk to 224 by 224 pixels in size (input size of EfficientNet-B1). By lowering the number of parameters to learn, max-pooling lowers the computational cost and offers fundamental translation invariance to the internal representation. For fully connected layers, Adam's optimizer employed a learning rate of 0.001, L1 and L2 regularization with values of 0.006 and 0.016, respectively, and a Re-LU activation function. To prevent overfitting, the dropout rate of the final fully linked layer is set to 0.45. There are 40 iterations of training for the models, with a batch size of 40. Our experiment runs on an NVidia GeForce GTX 1080 Ti GPU with 8 GB of RAM and makes use of TensorFlow as the frontend and the Keras package as the backend.

B. The Results and Discussions

A total of 6020 photos are used to train the models, 752 images are used to validate them, and 753 test images are used to obtain the findings. The accuracy, sensitivity, specificity, precision, and F1-Score of the gathered data are summarized in Table (3), which shows that the recommended model surpasses all others and obtains the maximum degree of accuracy for three categorization criteria.

Table 3 indicates that the proposed model has good accuracy when utilizing the artificially augmented dataset (86.10%). The proposed model also generates findings with high sensitivity (87.24%) and accuracy (87.60%).

Table 3 : Pre-trained network classification results and recommended design. The bold number is the best outcome; the underlined value reflects the category's second-best performance.

Method	Accuracy (%)	Recall (%)	Precision (%)	F1-score (%)
<u>Xception</u>	<u>79.59</u>	<u>82.35</u>	<u>76.32</u>	<u>78.2</u>
InceptionV3	78.72	63.64	71.37	73.1
MobileNet	79.01	76.47	77.62	78.2
ResNet50	74.64	56.52	73.71	71.1
EfficientNetB1	86.1	87.24	87.6	89.32

To support ResNet50, InceptionV3, Mobile-Net, and Xception architectures are compared to the proposed design's performance. Our model enhances ResNet50 accuracy by 11.46 percent, InceptionV3 accuracy by 7.38 percent, Mobile-Net accuracy by 7.09 percent, and the original Xception architecture accuracy by 6.51 percent, as shown in Table 3.

Furthermore, the original Xception design (79.59 percent) outperforms ResNet50, InceptionV3, and MobileNet architectures in terms of performance. This is most likely due to residual blocks and the Xception architecture's mix of point-wise blocks, depth-wise convolutional layers, and inception modules, which outperform Mobile-Net's depth-wise, point-wise convolutional layers, ResNet50's residual blocks, and InceptionV3's inception modules. With (74.64) percent accuracy, (56.52) percent sensitivity, (73.71) percent precision, and a (71.1) percent f1-score, ResNet50 is the least accurate classifier. The results indicate that combining these modules is advantageous. Combining intermediate convolutional layers from the Xception architecture with auxiliary features can help with the extraction of additional discriminative qualities. Figure 5 shows the disparity between the actual and anticipated situations as predicted by the confusion matrix.

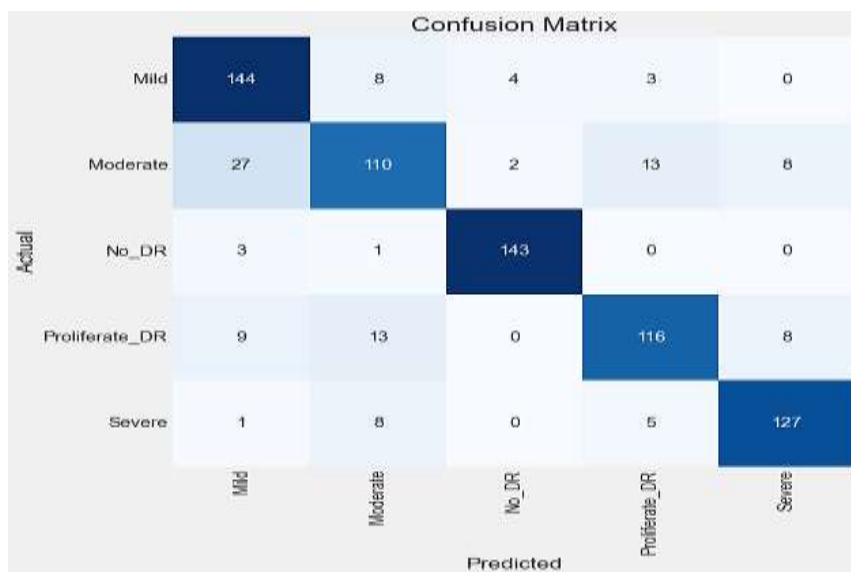


Figure 5: Confusion Matrix gives the prediction between the actual and

This confusion matrix gives a lot of information about the model’s performance. As usual, the diagonal elements are the correctly predicted samples. The lower the error rate and the more accurate the predictions, the larger the diameter of the results. To improve the model’s performance, one should focus on the predictive results in class 1, where a total of 110 samples in class 1 were classified correctly, in addition to the numbers in the red boxes of column 1, which were misclassified by the classifier, which is the highest misclassification rate among all the classes.

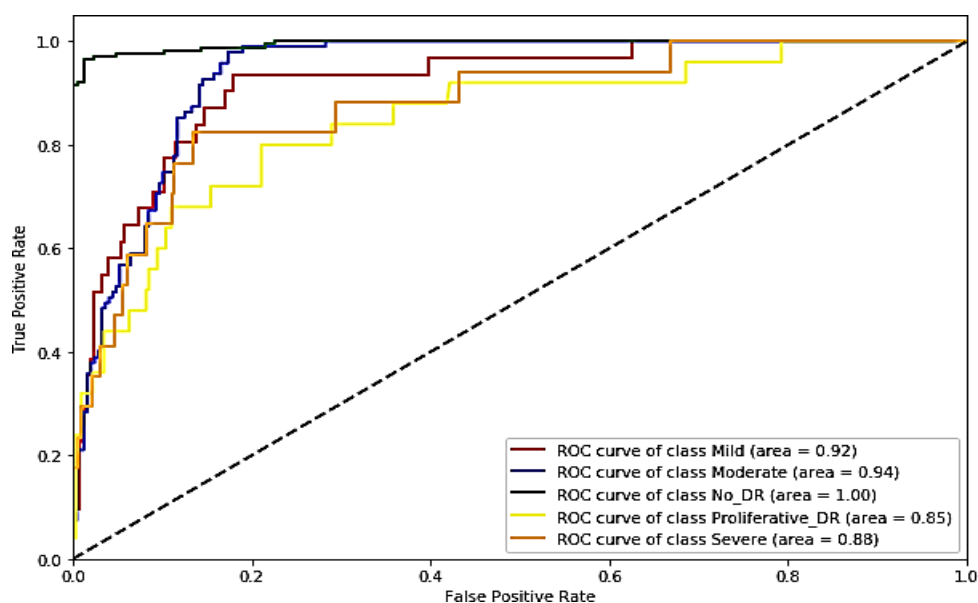


Figure 6: The suggested model's ROC curve for DR Screening using the APTOS dataset.

Figure 6 shows the ROC curve for the recommended model. The AUC for the No DR, Moderate, and Mild classes, according to this graphic, is 100 percent, 94.00 percent, and 92.00 percent, respectively. Severe and proliferative DR, on the other hand, received 88.00 and 85.00 percent, respectively. The uneven training sample, with 5% and 8% for these two groups, might

logically explain the low identification rate. Furthermore, certain fundus pictures' morphologies exhibit anatomical heterogeneity and shape variation, which makes it more challenging to identify unhealthy structures.

5. Conclusions

Diabetes mellitus (DM) is a type of diabetes that causes vision problems. This sickness may have no symptoms or just cause minor visual difficulties, but it can lead to blindness in the long run. Because the traditional approach for detecting DR is time-consuming, difficult, and expensive, several studies have been conducted to automate the procedure. Computer techniques have improved. For instance, DL and AI models have enhanced the likelihood of detecting DR early. Patients have a better chance of reducing and recovering from the risk of visual loss if they receive early screening. Technological developments in computer science, including deep learning (DL) models and artificial intelligence (AI), have boosted the odds of early DR detection. Patients will have a higher chance of recovering if they are discovered early, and the risk of visual loss will be lowered. The APTOS 2019 dataset was used to assess deep transfer learning models for medical DR detection. According to the literature, augmentation techniques were used to enhance and balance the dataset photographs in order to avoid overfitting (because they were very unbalanced). EfficientNetB1 was chosen as the deep transfer learning model in this work, and it was compared to Xception, InceptionV3, ResNet50, and MobileNet. According to overall testing accuracy and performance measures, the EfficientNetB1 model has the highest overall testing accuracy (86.1%), precision, and F1 score percentages (precision, recall, and F1 score). Future work will be done on cell phones in real-time (Android and iOS). The core IOT methodology employing DL will also be addressed, with multiple datasets and classification approaches.

References

- [1] N. H. S. Cho, J. E. Karuranga, S. Huang, Y. da Rocha Fernandes, J. D. Ohlrogge, A. W. Malanda, B., "IDF Diabetes Atlas: Global estimates of diabetes prevalence for 2017 and projections for 2045," *Diabetes Res Clin Pract*, vol. 138, pp. 271-281, Apr 2018, doi: 10.1016/j.diabres.2018.02.023.
- [2] N. Chakrabarty, "A Deep Learning Method for the detection of Diabetic Retinopathy," *IEEE*, pp. 1-5, 12 Apr 2018, doi: 978-1-5386-5002-8/18.
- [3] S. S. Sashank Sridhar, "Detection and Prognosis Evaluation of Diabetic Retinopathy using Ensemble Deep Convolutional Neural Networks," *IES*, pp. 78-85, 1 Nov 2020, doi: 978-7281-9530-8/20/.
- [4] J. P. Abhishek Deshpande, "Automated detection of Diabetic Retinopathy using VGG-16 architecture," *IRJET*, vol. 08, no. 03, pp. 2936-2940, 03 Mar 2021, doi: 2395-0072.
- [5] P. M. a. D. S. Borys Tymchenko, "Deep Learning Approach to Diabetic Retinopathy Detection," *arXiv*, pp. 1-9, 3 Mar 2020, doi: 2003.02261v1.
- [6] S. S. Nirmala, Purabi., "Computer Assisted Methods for Retinal Image Classification," *IGI Global*, pp. 233-255, 13 Sep 2017, doi: 10.4018/978-1-4666-8493-5.ch010.
- [7] S. H. K. Kassani, Peyman Hosseinzadeh Khazaeinezhad, Reza Wesolowski, Michal J. Schneider, Kevin A. Deters, Ralph, "Diabetic Retinopathy Classification Using a Modified Xception Architecture," *presented at the IEEE International Symposium on Signal Processing and Information Technology (ISSPIT)*, 2019.
- [8] kaggle. "Asia Pacific Tele-Ophthalmology Society (APTOS) 2019 Blindness Detection " <https://www.kaggle.com/c/aptos2019-blindness-detection/> (accessed).
- [9] P. H. K. Sara Hosseinzadeh Kassani, Michal J. Wesolowski, Kevin A. Schneider, Ralph Deters, "Breast Cancer Diagnosis with Transfer Learning and Global Pooling," *IEEE*, pp. 519-524, 23 Feb 2019, doi: 978-1-7281-0893-3/19/.
- [10] A. Rivela, "Why you should(n't) build your own game engine," *presented at the ACM SIGGRAPH 2019 Talks*, 2019.
- [11] S. H. K. Hosseinzadeh Kassani, P., "A comparative study of deep learning architectures on

- melanoma detection," *Tissue Cell*, vol. 58, pp. 76-83, Jun 2019, doi: 10.1016/j.tice.2019.04.009.
- [12] R. M. Sarki, Sandra Ahmed, Khandakar Wang, Hua Zhang, Yanchun., "Convolutional neural networks for mild diabetic retinopathy detection: an experimental study," *bioRxiv*, pp. 1-12, 28 Aug 2019, doi: 10.1101/763136.
- [13] W. B. Debiao Zhang, Xiangqian Wu. , "Diabetic Retinopathy Classification using Deeply Supervised ResNet," *IEEE*, pp. 1-6, 18 Oct 2017, doi: 978-1-5386-0435-9/17/.
- [14] H. C. Pratt, Frans Broadbent, Deborah M. Harding, Simon P. Zheng, Yalin., "Convolutional Neural Networks for Diabetic Retinopathy," *Procedia Computer Science*, vol. 90, pp. 200-205, 2016, doi: 10.1016/j.procs.2016.07.014.
- [15] S. B. Shivashish Naithani, Dhiraj Kumar., "Automated Detection of Diabetic Retinopathy using Deep Learning," *IRJET*, vol. 06, pp. 2945-2947, Apr 2019 2019, doi: 2395-0072.
- [16] D. S. Doshi, Aniket Sidhpura, Deep Gharpure, Prachi, "Diabetic retinopathy detection using deep convolutional neural networks," *presented at the International Conference on Computing, Analytics and Security Trends (CAST)*, 13 Dec, 2016.
- [17] S. Mohammadian., "Comparative Study of Fine-Tuning of Pre-Trained Convolutional Neural Networks for Diabetic Retinopathy Screening," *ICBME*, pp. 1-6, 1 December 2017, doi: 978-1-5386-3609-1/17.
- [18] S. A.-Z. Saad ALBAWI, "Understanding of a Convolutional Neural Network," *ICET*, pp. 1-6, 11 Jun 2017, doi: 978-1-5386-1949-0/17/.
- [19] V. B. P. Marius, L. Perescu-Popescu and N. Mastorakis., "Multilayer Perceptron and Neural Networks," *WSEAS Transactions on Circuits and Systems*, vol. 8, no. 7, pp. 579-588, July 2009 2009.
- [20] Q. V. L. Mingxing Tan "EfficientNet: Rethinking Model Scaling for Convolutional Neural Networks," *arXiv*, pp. 1-11, 11 Sep 2020, doi: 1905.11946v5
- [21] V. Agarwal, "Complete Architectural Details of all EfficientNet Models," pp. 1-15.
- [22] F. Chollet, "Xception: Deep Learning with Depthwise Separable Convolutions," *presented at the 2017 IEEE Conference on Computer Vision and Pattern Recognition (CVPR)*, 2017.
- [23] A. G. H. M. Z. B. C. D. Kalenichenko., "MobileNets: Efficient Convolutional Neural Networks for Mobile Vision Applications," *arXiv*, pp. 1-9, 17 Apr 2017, doi: 1704.04861v1.
- [24] G. D. a. L. W. Cahill, "An Adaptive Gaussian Filter For Noise Reduction and Edge Detection," *IEEE*, pp. 1615-1619, 12 Jun 1994, doi: 0-7803- 1487-5/94\$04.00.
- [25] A. I. Buslaev, Vladimir I. Khvedchenya, Eugene Parinov, Alex Druzhinin, Mikhail Kalinin, Alexandr A., "Albumentations: Fast and Flexible Image Augmentations," *Information*, vol. 11, no. 2, pp. 1-20, 5 Nov 2020, doi: 10.3390/info11020125.
- [26] C. G. E. Gaussier, "A Probabilistic Interpretation of Precision, Recall and F-Score, with Implication for Evaluation.," *LNISA*, vol. 3408, pp. 345–359, 3 Mar 2010.
- [27] E. S. D. Nasser, Faten Abd Ali, "Diagnosis and Classification of Type II Diabetes based on Multilayer Neural Network," *Iraqi Journal of Science*, pp. 3744-3758, 14 April 2021, doi: 10.24996/ij.s.2021.62.10.33.
- [28] M. M. S. Rahma, Aymen Dawood, "Heart Disease Classification–Based on the Best Machine Learning Model," *Iraqi Journal of Science*, pp. 3966-3976, 30 Sep 2022, doi: 10.24996/ij.s.2022.63.9.28.
- [29] S. N. J. Firke, Ranjan Bala, "Convolutional Neural Network for Diabetic Retinopathy Detection," *presented at the 2021 International Conference on Artificial Intelligence and Smart Systems (ICAIS)*, 2021.
- [30] E. Team, "How to evaluate you model using the Confusion Matrix."